Drainage evolution in the Margaritifer Sinus region, Mars

John A. Grant
Center for Earth and Planetary Studies, National Air and Space Museum, Smithsonian Institution, Washington, D. C., USA

Timothy J. Parker
Jet Propulsion Laboratory, Pasadena, California, USA

Received 25 September 2001; revised 8 March 2002; accepted 30 April 2002; published 21 September 2002.

[1] Margaritifer Sinus, Mars, records a complex history of water transport, storage, and release extending from the late Noachian into at least the mid-Hesperian. Collection, transport, and discharge of water were accomplished by systems of differing character flanking opposite sides of the Chryse Trough. Drainage on the western side of the trough was via the segmented Uzboi-Ladon-Margaritifer mesoscale outflow system that heads in Argyre Basin and incises and fills as it crosses ancient multiringed impact basins. By contrast, Samara and Parana-Loire Valles, two of the largest and best integrated valley systems on Mars, dominated drainage on the eastern trough flank. Valley morphometry suggests formation was due to precipitation-recharged groundwater sapping. All systems discharged into Margaritifer Basin, located along the Chryse Trough axis, and caused ponding that persisted into the early Hesperian. The Uzboi-Ladon-Margaritifer system dominated discharge that was coincident with widespread geomorphic activity on Mars. As channel and valley formation ended, some water in Margaritifer Basin infiltrated the subsurface. Collapse and release of water began shortly thereafter and persisted into mid-Hesperian times, thereby forming Margaritifer and Iani Chaos and incising Ares Vallis. *INDEX TERMS:* 6225 Planetology: Solar System Objects: Mars; 5415 Planetology: Solid Surface Planets: Erosion and weathering; 5470 Planetology: Solid Surface Planets: Surface materials and properties; 5407 Planetology: Solid Surface Planets: Atmospheres—evolution; 1860 Hydrology: Runoff and streamflow; *KEYWORDS:* Mars, water, valleys, channels, rainfall, sapping

Citation: Grant, J. A., and T. J. Parker, Drainage evolution in the Margaritifer Sinus region, Mars, *J. Geophys. Res.*, *107*(E9), 5066, doi:10.1029/2001JE001678, 2002.

1. Introduction

[2] Valleys and channels on Mars were first identified in Mariner 6 and 7 images [*Schultz and Ingerson*, 1973] and understanding the processes responsible for their formation has been the focus of considerable study ever since [*Carr*, 1981, 1996; *Baker*, 1982; *Mars Channel Working Group*, 1983; *Baker et al.*, 1992]. Similarly, possible relationships in timing or formation processes between valley systems, meso-outflow channels, and large outflow systems often remain uncertain [*Baker*, 1982]. Understanding such relationships, however, is the key to constraining the past Martian hydrologic cycle by determining how, when, and where water moved and was stored.

[3] The wealth of new data from the Mars Global Surveyor spacecraft (MGS) coupled with data from prior missions permit evaluating drainage systems on scales ranging from basin-wide at moderate resolution (100–200 m) to local scale at high resolution (5–10 m). The current study examines drainage systems in the Margaritifer Sinus region and provides new insight into the history of water collection, transport, and storage on Mars.

0148-0227/02/2001JE001678$09.00

2. Drainage Systems in Margaritifer Sinus

[4] The Margaritifer Sinus region of Mars (0°–45°W, 0°–30°S) is located near the eastern end of Valles Marineris (Figure 1), straddles the Chryse Trough [*Saunders*, 1979; *Baker*, 1982; *Phillips et al.*, 2000, 2001], and preserves numerous well-preserved valleys and channels [*Carr*, 1981; *Baker*, 1982; *Mars Channel Working Group*, 1983; *Carr and Chuang*, 1997; *Grant*, 2000].

[5] The segmented Uzboi-Ladon-Margaritifer meso-outflow system (ULM) heads south of Argyre Basin [*Parker*, 1985, 1994] and is characterized by incised trunk sections separated by depositional plains filling ancient multiringed impact basins (Figure 2) [*Saunders*, 1979; *Schultz et al.*, 1982]. Collectively, ULM drains over $\sim 11 \times 10^6$ km^2 or about 9% of Mars [*Banerdt*, 2000; *Phillips et al.*, 2001] along and south of the western flank of the Chryse Trough (Figure 1). By contrast, Samara and Parana-Loire Valles (Figure 1) drain the eastern side of the Chryse Trough (Figures 1 and 2), head at elevations of 1–2 km (MOLA datum [see *Smith et al.*, 1999]), and cover an area exceeding 540,000 km^2 or $\sim$0.5% of Mars. Relative to ULM, Samara and Parana-Loire Valles are well integrated and continuously incised.

[6] The ULM system and Samara and Parana-Loire Valles all debouch into the Margaritifer Basin confluence

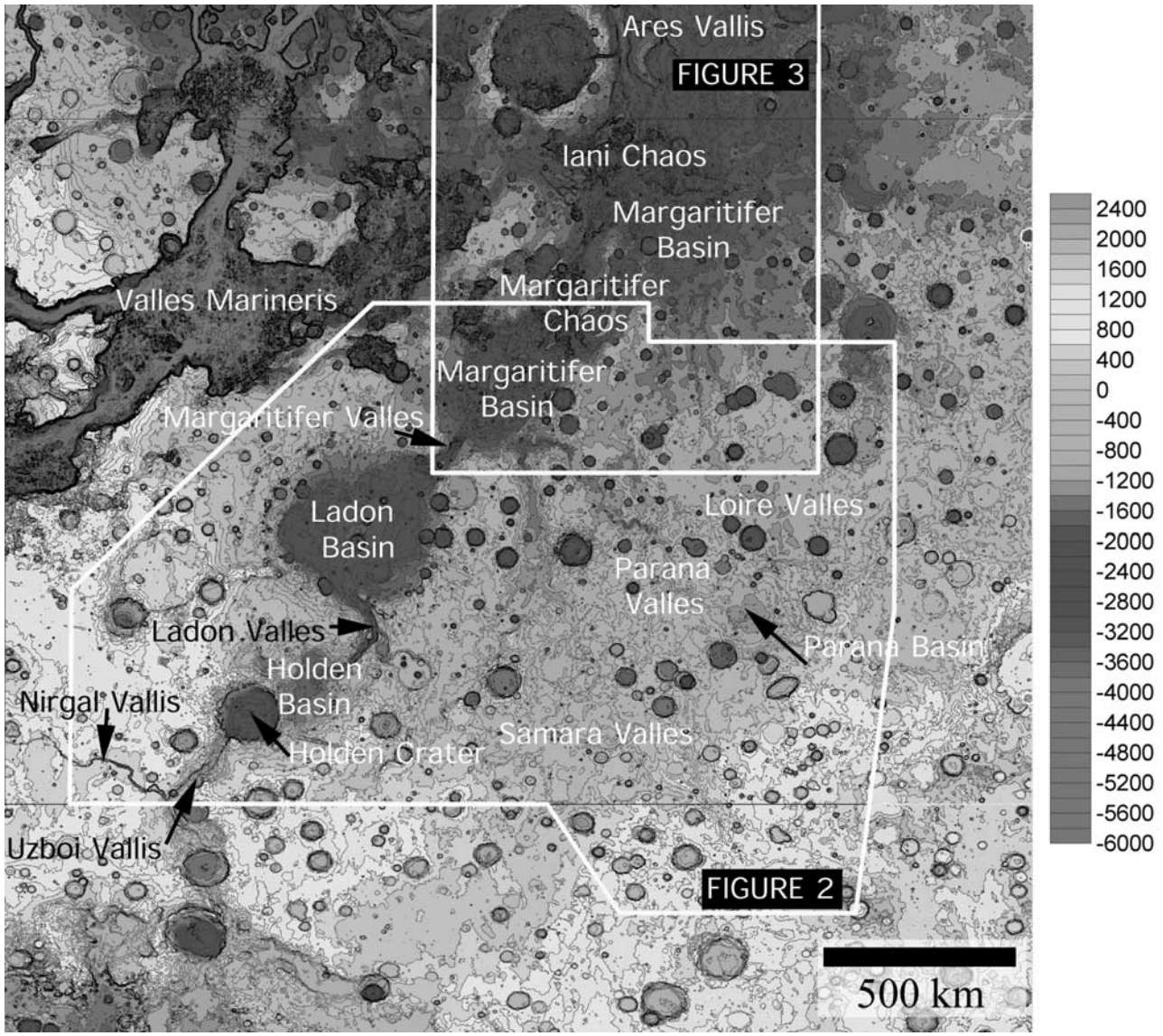

Figure 1. Topography of Margaritifer Sinus and northern Argyre from 5°N to 45°S and 0°W to 45°W. Labeled features are discussed in text. Axis of the Chryse Trough runs approximately through the center of the figure from top to bottom. North is toward the top and figure was generated from the 64 cell/degree MOLA grid. Approximate limit of drainage divide map in Figure 2 and extent of MOLA topography displayed in Figure 3 are indicated.

plain along the axis of the Chryse Trough and immediately south of Margaritifer Chaos and Ares Vallis [*Grant*, 1987; *Grant and Parker*, 2000, 2001]. Smooth plains punctuated by "islands" of cratered uplands characterize the depositional basin (Figure 3) whose northeastern extent is indistinct, but reaches at least to the head of Ares Vallis [*Edgett and Parker*, 1997; *Grant and Parker*, 2001].

[7] The juxtaposition of the Margaritifer Sinus drainages (Figures 2 and 3) leads to questions related to possible relationships between the processes and timing of formation. The current study focuses on the history of water movement and storage in the Margaritifer Sinus region based upon geologic mapping, analysis of MGS Mars Orbiter Camera (MOC) and Mars Orbiter Laser Altimeter (MOLA) data, and stereo mapping using Viking Orbiter images (mostly 150–250 m/pixel). Next, a summary of the geologic history of the Margaritifer Sinus region provides context for understanding the evolution of the channels and valleys. This is followed by descriptions of the ULM, Samara and Parana-Loire Valles, and consideration of evolutionary scenarios. Finally, a discussion of Margaritifer Basin details the possible fate of the water flowing through these systems.

3. Geologic Events in Margaritifer Sinus

[8] Geologic mapping enables the timing of channel and valley formation to be constrained relative to other major geologic events [*Parker*, 1985, 1994; *Grant*, 1987, 2000]. Our mapping builds upon prior results [e.g., *Saunders*, 1979; *Hodges*, 1980; *Scott and Tanaka*, 1986] and incorporates more than 100 sets of crater statistics to define

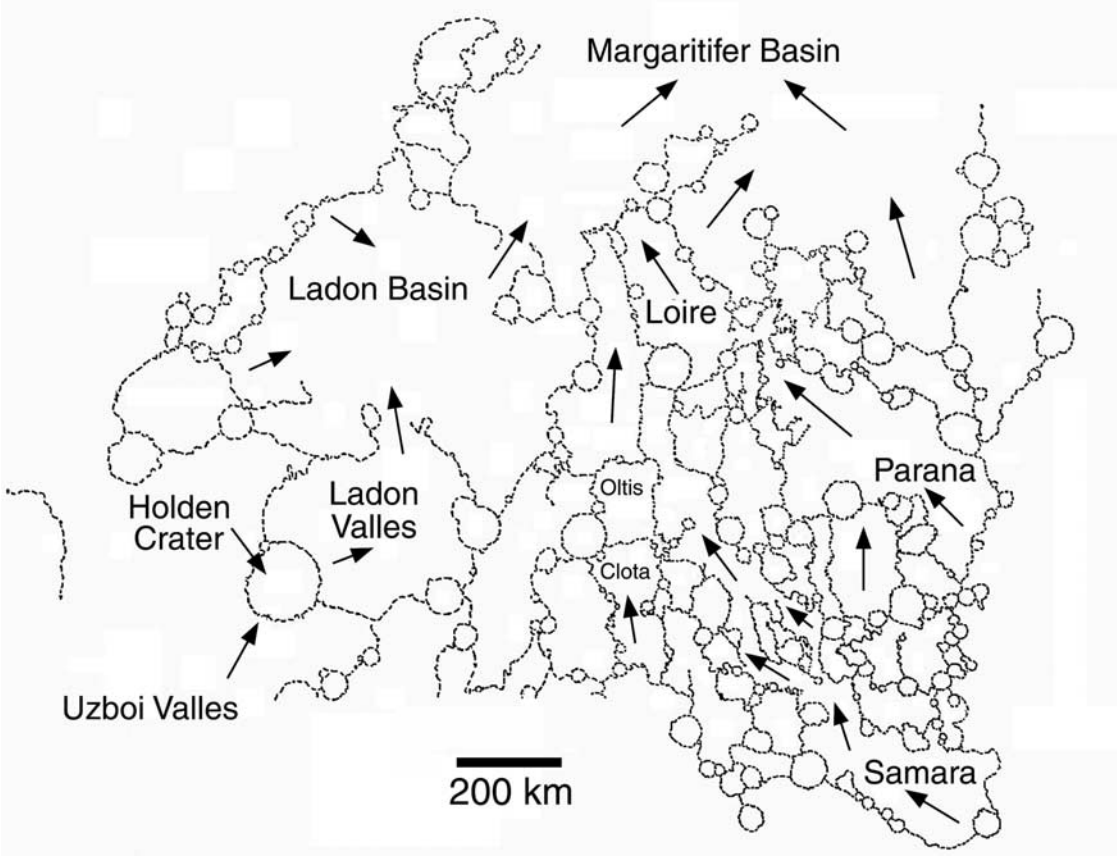

Figure 2. Major drainage basins in the Margaritifer Sinus region defined using stereo pairs of Viking Orbiter Images and confirmed via review of MOLA data. North is toward the top and arrows denote local drainage direction. Labels correspond to features denoted in Figure 1.

relative ages (given as the N5 age for the number of craters larger than or equal to 5 km in diameter per 1,000,000 km^2). Mapping methods and techniques for generating crater statistics are described by *Parker* [1985] and *Grant* [1987] and are consistent with *Ford et al.* [1993] and *Tanaka et al.* [1994].

[9] As summarized from *Grant* [2000] and in Figure 4, cratered upland inliers and the degraded Holden, Ladon, and Noachis multiringed impact basins [*Saunders*, 1979; *Schultz et al.*, 1982; *Frey et al.*, 2001] are the oldest features in Margaritifer Sinus. Relatively competent materials interpreted to be of sedimentary and/or volcanic origin (on the basis of preserved wrinkle ridges and occasionally lobate boundary morphology) were emplaced during four resurfacing events and bury much of the cratered uplands. The first three resurfacing events were regional in extent and predate evolution of ULM and the valleys (Figure 4). The first two occurred in the early Noachian, with the second ending at an N5 age of 1400. The third ceased during the late Noachian (N5 of 300) coincident with waning highland volcanism [*Wise et al.*, 1979; *Scott and Tanaka*, 1986]. A fourth, more localized resurfacing event extended into the middle Hesperian (N5 ages 200 to 70).

[10] Formation of Samara and Parana-Loire Valles, ULM, and filling of associated depositional sinks all occurred from late Noachian (N5 of 300) into the early Hesperian (N5 of 150), concurrent with widespread gradation elsewhere on Mars [*Grant and Schultz*, 1990, 1993a; *Grant*, 2000]. The timing of channel and valley formation is based on the fact that they incise and are buried by materials associated with the third and fourth resurfacing events, respectively (Figure 5), and interpretation of crater statistics from deposits filling Ladon and Parana Basins (Figures 1 and 4).

[11] Initial collapse of Margaritifer and Iani Chaos (Figure 1) disrupted valley and channel deposits in Margaritifer Basin and further supports cessation of channel and valley formation by an N5 age of around 150 (Figure 4). Previous studies indicate these chaos regions served as the source for Ares Vallis [*Carr*, 1979; *Carr and Clow*, 1981; *Rotto and Tanaka*, 1995], but that the bulk of the collapse occurred later in time (Figures 3 and 4) [see *Masursky et al.*, 1977; *Carr*, 1979; *Rotto and Tanaka*, 1995]. Our results contradict an earlier conclusion that formation of ULM extended into the middle to perhaps late Hesperian [*Rotto and Tanaka*, 1995].

[12] This summary of events in Margaritifer Sinus provides a framework for discussing the evolution of the ULM and Samara and Parana-Loire systems, respectively.

4. Evolution of the ULM System

4.1. Overview

[13] Incised segments with intervening depositional basins characterize the ULM system (Figures 1 and 2)

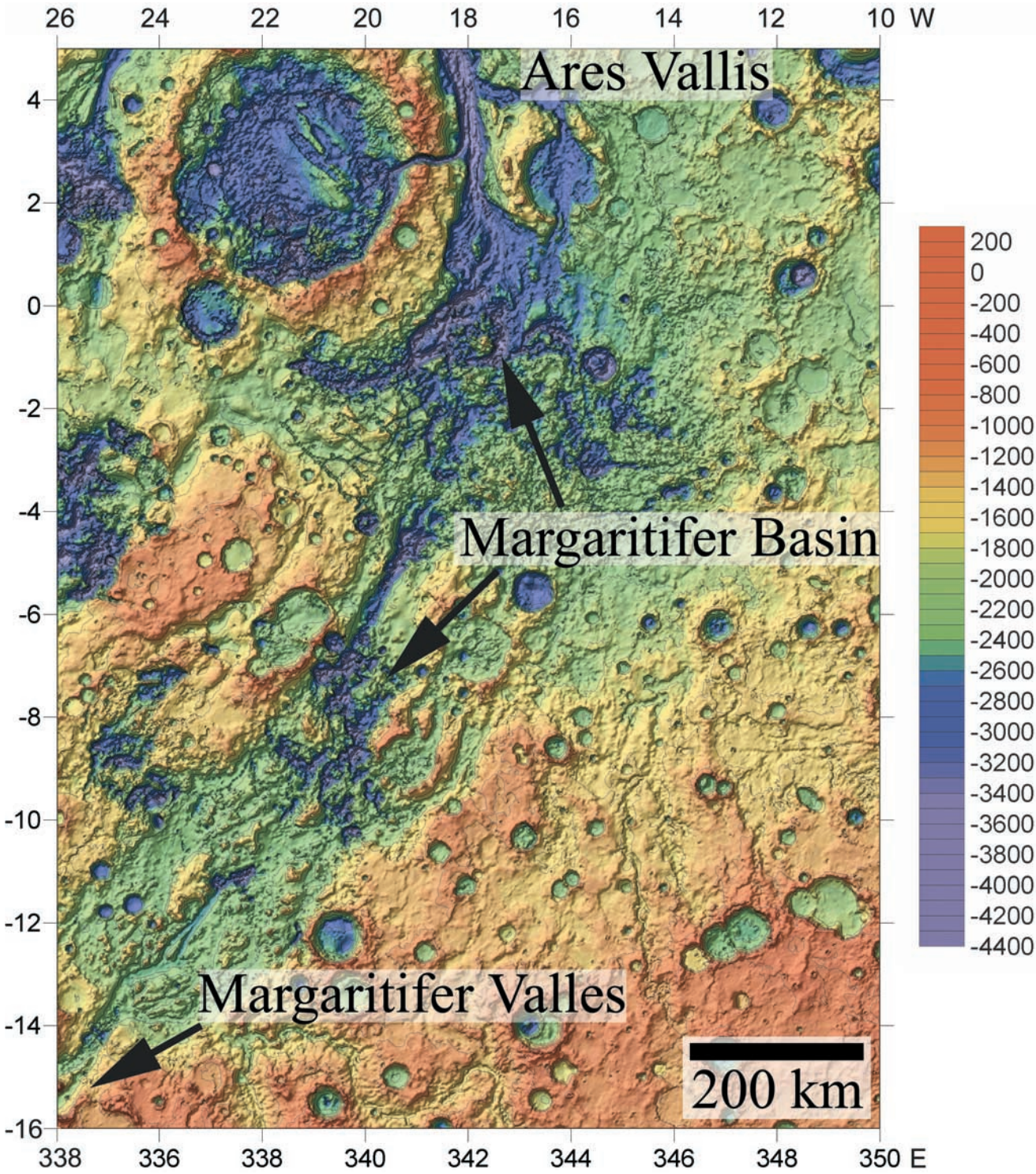

Figure 3. Gridded MOLA data (64 cells/degree) displayed as shaded relief for Margaritifer Basin (from outlet of Margaritifer Valles to head of Ares Vallis, approximately 5°N to 16°S and 10°W to 26°W, image center is 5.4°S, 18.7°W). North is toward top of the image. Elevations range from below −2.5 km (MOLA datum) in blue and purple to between −2 and −1 km (green/yellow) to above −1.5 km (red).

[*Boothroyd*, 1983; *Parker*, 1985]. The location and orientation of the incised reaches is influenced by structure associated with the Holden, Ladon, and Margaritifer multiringed impact basins [*Schultz et al.*, 1982], whereas deposition characterizes the interiors of these basins (Figures 1 and 2). ULM experienced multiple discharge events as indicated by terraces along Uzboi Vallis, at least four terraces along Ladon Valles (Figure 6) [*Boothroyd*, 1983; *Parker*, 1985; *Grant*, 1987], and a complex sequence of distributaries and terraces at the mouth of Margaritifer

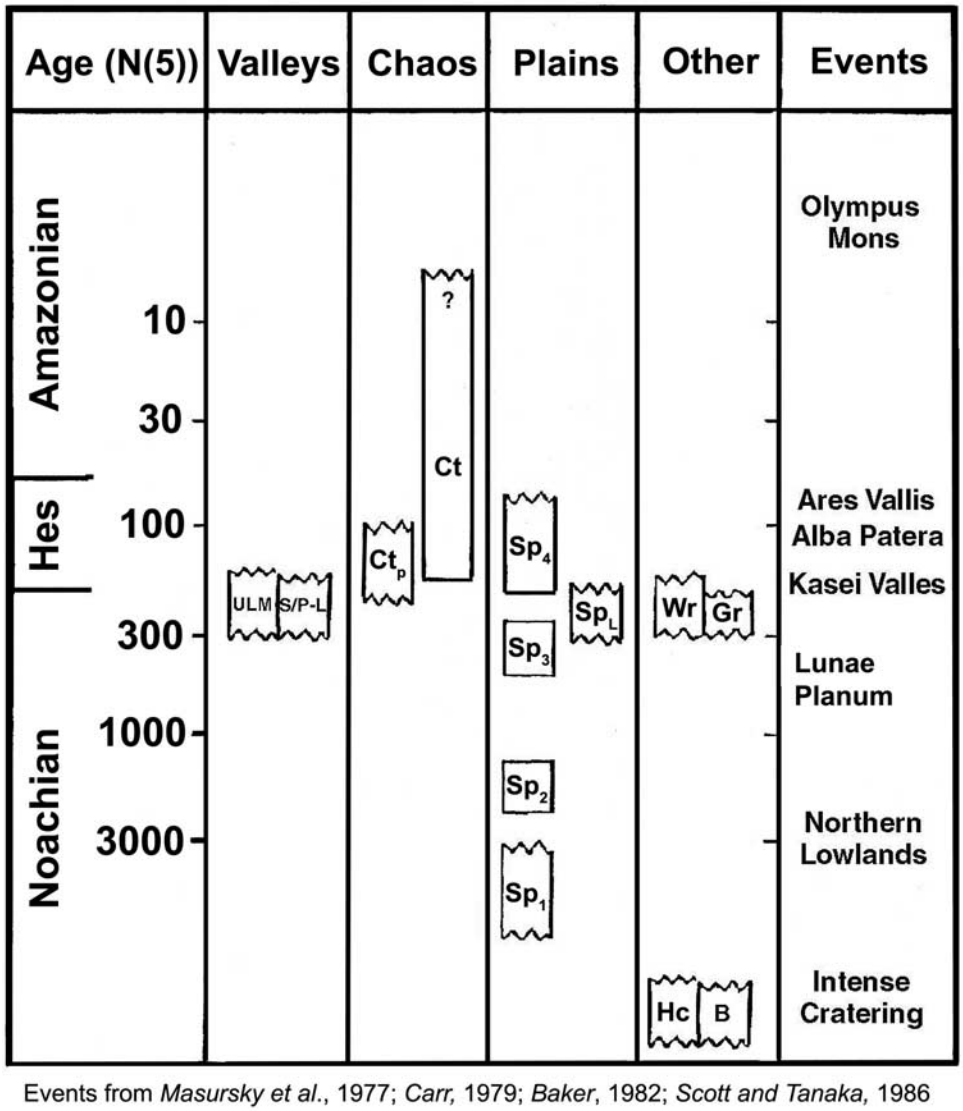

Figure 4. Summary of the geologic history in the Margaritifer Sinus region modified from *Grant* [2000]. N5 age gives the relative age of a surface based on the normalized number of craters larger than 5 km in diameter per 1,000,000 km^2. ULM is the Uzboi-Ladon-Margaritifer Valles meso-outflow system, S/P-L is Samara and Parana-Loire Valles. Ct and Ct_p refer to chaotic terrain and positive relief chaotic terrain (in Parana Basin), respectively. Hc and B refer to the approximate interval of cratered upland and multiringed basin formation. Sp_{1-4} refer to resurfacing events of probable sedimentary and/or volcanic origin, whereas Sp_L identifies the time of infilling in Ladon Basin. Wr and Gr denote the timing of deformation related to wrinkle ridge and graben formation. Selected events occurring on Mars are from *Scott and Tanaka* [1986].

Valles. Both the Ladon and Margaritifer segments display a prominent, deeply incised central channel, thereby implying flow became focused during discharge from upstream basins.

[14] The floor of Ladon Basin is flat (maximum relief 0.27 km over 350 km) and grades from the mouth of Ladon Valles to the head of Margaritifer Valles. Evidence for comparable low depositional relief across Holden Basin was destroyed by formation of crater Holden and adjacent chaotic terrain to the northeast. Fill within both Holden and Ladon basins, however, confirms occurrence of coarse layering (Figures 7a and 7b) and supports the contention that the ULM system experienced multiple discharges.

4.2. Estimates of Discharge Along the ULM System

[15] Constraining discharge through the ULM system is key to understanding how much water may have been delivered to Margaritifer Basin and the source region for Ares Vallis. Availability of MGS MOLA data permits measurement of channel gradient and cross-section that can be used in deriving estimates of mean velocity (V) and ultimately discharge (Q). Mean velocity calculations

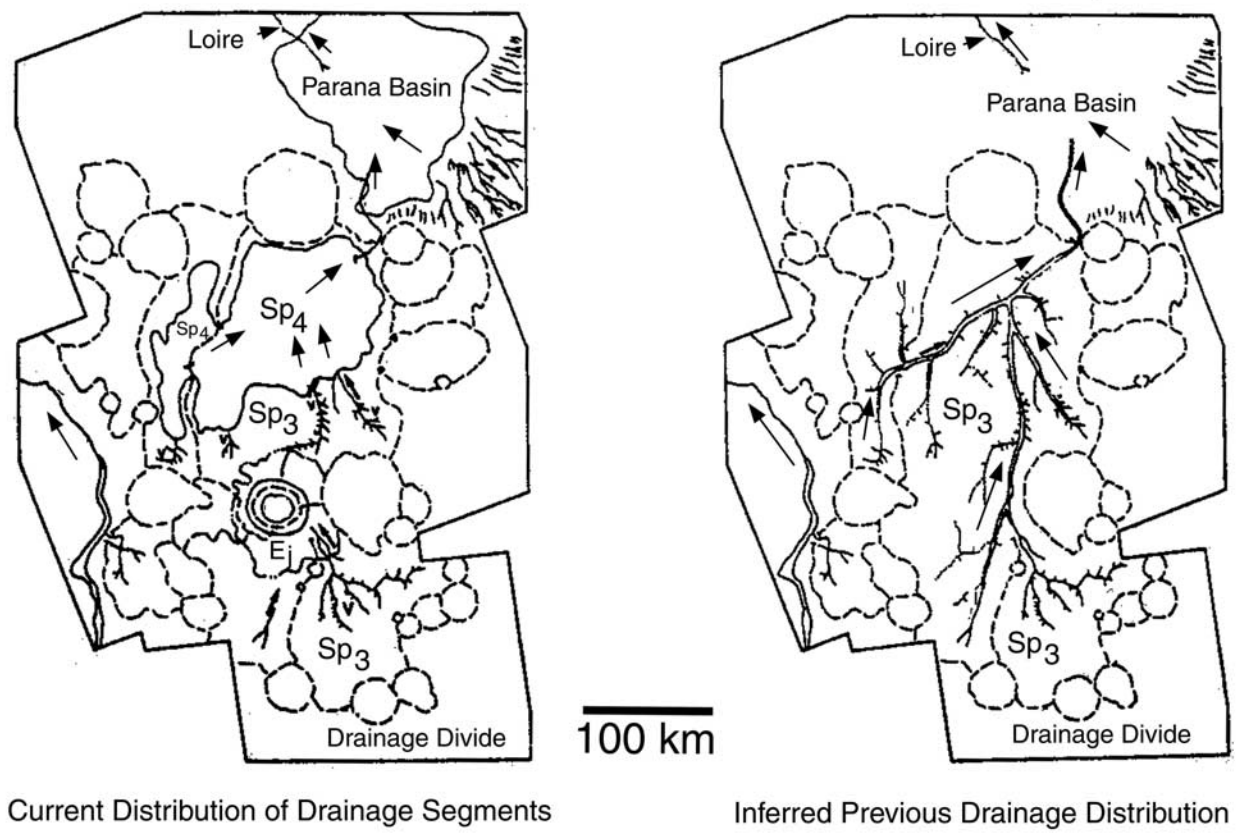

Figure 5. Geomorphic map and hypothesized reconstruction of original drainage distribution for a portion of MTM quadrangle −25012. Impacts and a fourth resurfacing event destroyed some drainage segments, thereby suggesting the original drainage density was greater than currently preserved. Mapping completed at a scale of 1:500,000 and unit designations refer to events described in Figure 4. The area is bounded by 22°S, 31°S, 10.5°W, and 16.5°W.

utilize a modified version of the semi-empirical Manning equation [*Carr*, 1979; *Komar*, 1979; *Baker*, 1982] where:

$$V = \frac{0.5}{n} D^{2/3} S^{1/2} \quad (1)$$

V is the mean flow velocity, n is the Manning roughness coefficient, D is the depth of flow, and S is the gradient of the channel floor. The terrestrial form of the equation has been modified to account for the lower Martian gravity by decreasing the relative magnitude of n [*Komar*, 1979].

[16] Availability of MOLA data enables accurate definition of channel gradient, but estimating channel cross-section is less precise because the depth of water that flowed in the channels is poorly constrained. Although channel relief indicates down-cutting of ~1.0 and ~0.8 kilometers for Ladon and Margaritifer Valles, respectively, analogy with terrestrial systems (e.g. the Niagara River Gorge) implies the maximum depth of flow within the channels was much less. To best measure flow in Ladon and Margaritifer Valles, channel slopes and cross-sections were derived using multiple profiles (Figures 8a and 8b, Table 1).

[17] Measured slopes along the channel thalwegs average 0.0008 (0.046°) and 0.0006 (0.034°) for Ladon and Margaritifer Valles, respectively (Table 1), whereas Manning roughness values are based on prior estimates for Martian outflow systems [*Carr*, 1979; *Komar*, 1979; *Baker*, 1982]: the assumed value of 0.04 for n is approximately equivalent to the average roughness along a mountain stream [*Ritter et al.*, 1995]. Flow depths were estimated where possible using the difference in elevation from the channel bottom to the lowest detectable terrace and yields depths of 28 to 88 m (Figure 9, Table 1), broadly consistent with that estimated for the larger outflow systems on Mars and the Channeled Scabland on the Earth [*Baker and Nummedal*, 1978; *Carr*, 1979; *Baker*, 1982].

[18] Inclusion of channel slope and depth of flow estimates in the modified Manning equation (1) yields mean flow velocities of 3.2–6.7 m/sec and 2.5–5.3 m/sec for Ladon and Margaritifer Valles, respectively (Table 1). By way of comparison, these velocities are low relative to estimates for the larger Martian outflow channels, less than those derived for the Channeled Scabland, but equivalent to or above velocities measured in the Mississippi [*Baker and Nummedal*, 1978; *Carr*, 1979; *Komar*, 1979; *Baker*, 1982; *Craddock and Tanaka*, 1995].

[19] First order estimates of discharge (Q) for the ULM system can be derived using:

$$Q = VA \quad (2)$$

where V equates to the mean velocities derived above and A is the channel cross-sectional area (assumed to be

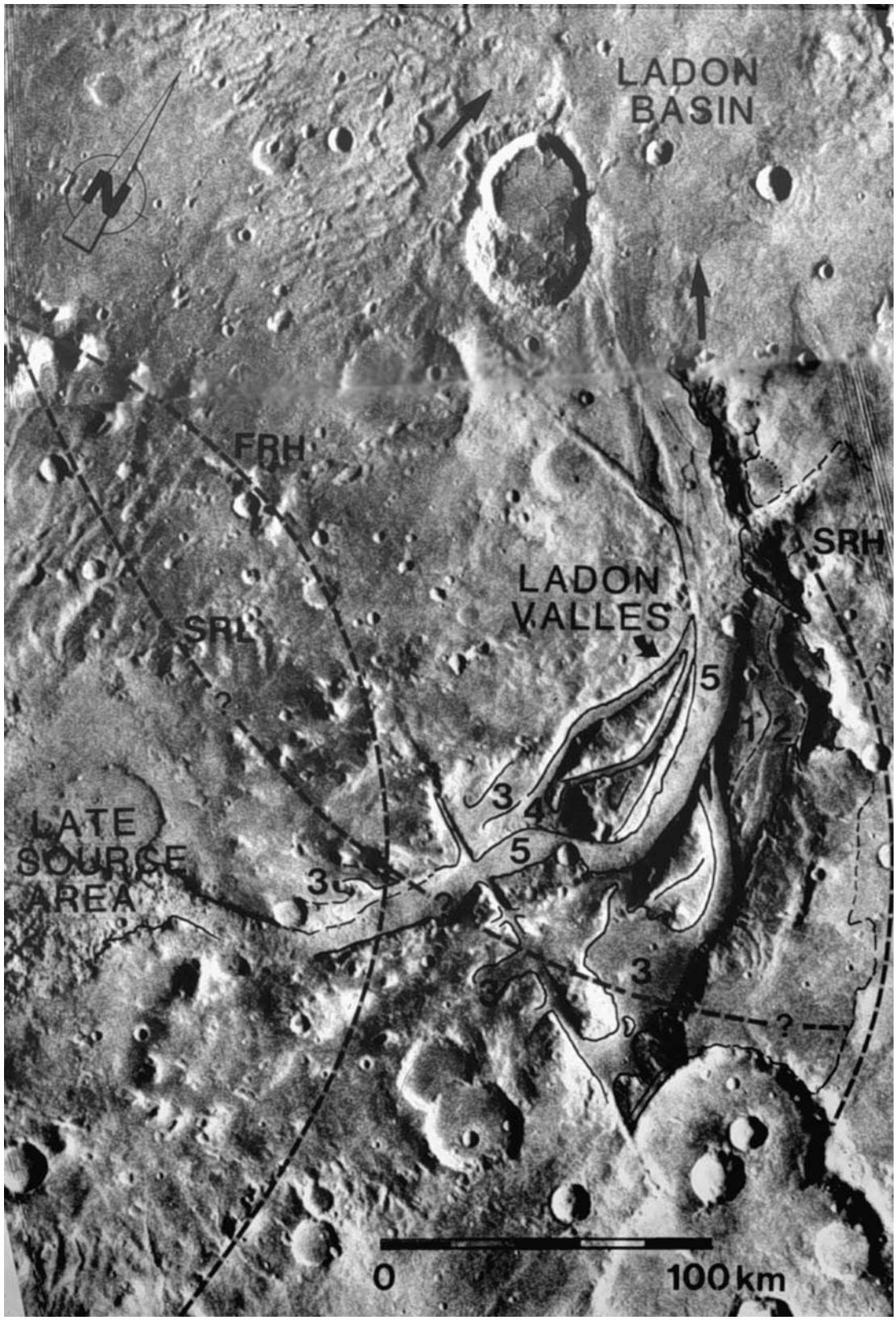

Figure 6. Viking image mosaic of Ladon Valles and vicinity. The system displays four terraces (labeled 1–4) and a prominent central channel (labeled 5) that heads in a small area of chaotic terrain in Holden Basin on the northeast margin of Holden crater. The system drains northeast across the inner rings of Holden and Ladon Basins before turning more northwesterly and debouching into Ladon Basin. Dashed lines mark the approximate location of the first (FRH) and second (SRH) rings of the Holden multiringed impact basin and the second (SRL) ring of the Ladon multiringed impact basin [from *Schultz et al.*, 1982].

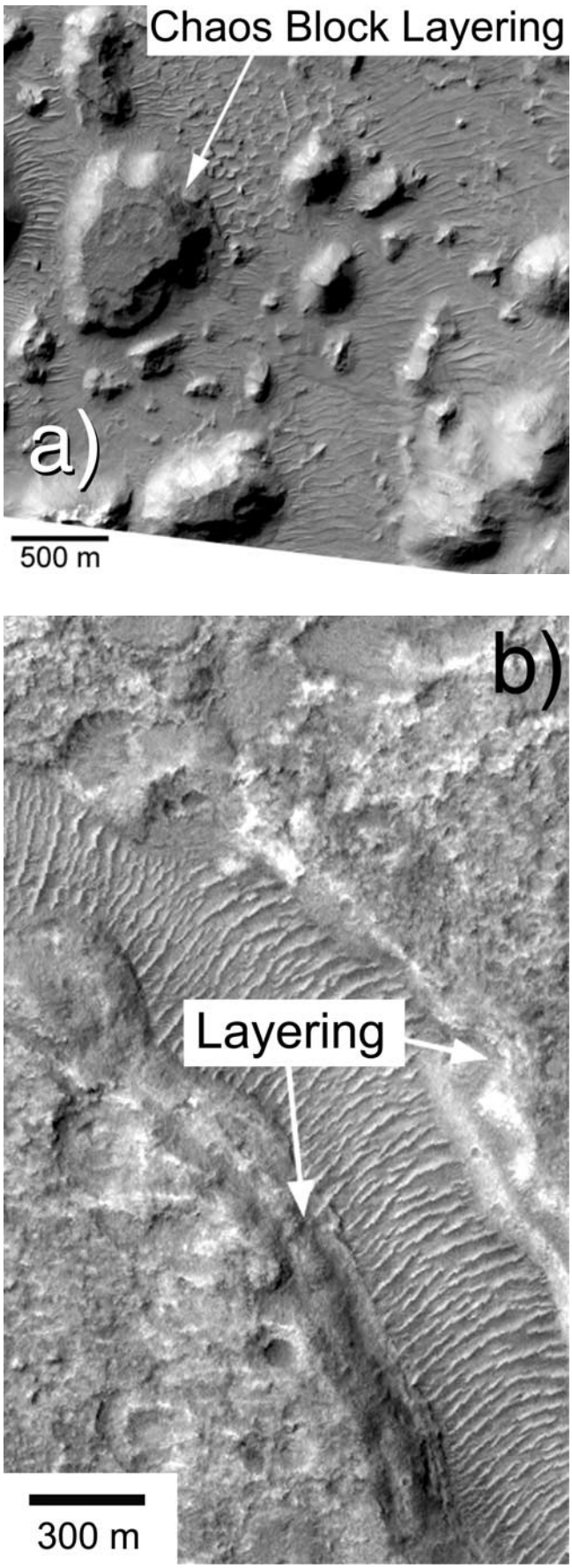

rectangular). Channel width was measured at the level of the terraces used in estimation of depth (Table 1). Resultant discharge estimates range over more than an order of magnitude, but most are between approximately 150,000 m^3 sec^{-1} and 450,000 m^3 sec^{-1} (Table 1). These estimates are 5–10 times higher than the discharge of the Mississippi river [*Komar*, 1979], on the lower end of discharge estimates for the Channeled Scabland [*Baker and Nummedal*, 1978; *Baker*, 1982], and generally near the low end or below estimates for the Martian outflow channels [*Carr*, 1979; *Komar*, 1979; *Baker*, 1982]. For example, estimated discharge from Ares Vallis was between 1.5×10^6 and 70×10^6 m^3 sec^{-1} [*Carr*, 1979; *Baker*, 1982].

[20] It is necessary to point out uncertainties involved in the estimates of velocity and discharge. For example, terraces may be mis-identified (Figure 9) and derived flow depths are maximized because it is unlikely that flow reached the terrace as the channel down-cut to the present base. Further uncertainty relates to the assumed rectangular channel cross-section. Nevertheless, the estimates are probably a reasonable proxy of first-order flow.

[21] While the ultimate source of most water transported through the ULM remains somewhat ambiguous, it must have been voluminous. Moreover, broad similarity in the estimated discharge from Ladon and Margaritifer Valles, layering in Ladon and Holden basin-fill, and graded alluvium from the mouth of Ladon to the head of Margaritifer Valles suggests that segments were simultaneously active. Hence, it is likely that the confluence plain at the mouth of Margaritifer Valles and Margaritifer Basin would have been repeatedly inundated to a depth of 100s of meters.

4.3. Late Stage Discharge and Formation of Crater Holden

[22] The formation of the ~140 km diameter crater Holden (26.0°S, 34.2°W; Figure 1) interrupted the ULM system and temporarily halted through-system discharge. Nevertheless, waning flow in Uzboi Vallis, dominated by discharge from the Nirgal Vallis tributary (30°S, 38°W), eventually breached the southern crater rim, resulting in ponding and deposition [*Parker*, 1985]. In contrast to earlier ULM discharge responsible for deposition of coarsely layered sediments in Holden and Ladon basins, flow into crater Holden led to extensive, finely layered deposits (Figure 10a) [*Grant and Parker*, 2000, 2001; *Malin and Edgett*, 2000]. The continuity of the layers and their flat-lying character strongly supports an origin related to deposition into standing water because facies deposited by alternate processes are typically less continuous.

[23] Late flow into crater Holden and associated deposition created wedge-shaped alluvial deposits that grade away

Figure 7. (opposite) Coarse layering in sediments filling Holden Basin (a) and Ladon Basin (b). Exposures in Holden Basin are in chaotic terrain whose formation contributed to late stage discharge along Ladon Valles. Exposures in Ladon Basin gained via fractures cutting the basin fill. Figure 7a is part of MOC image M0003055, centered at 24.6°S, 31.0°W, with 2.8m/pixel resolution. Figure 7b is part of MOC image M0204245, centered at 17.5°S, 30.7°W, with 2.8 m/pixel resolution. North is toward the top of both of both images.

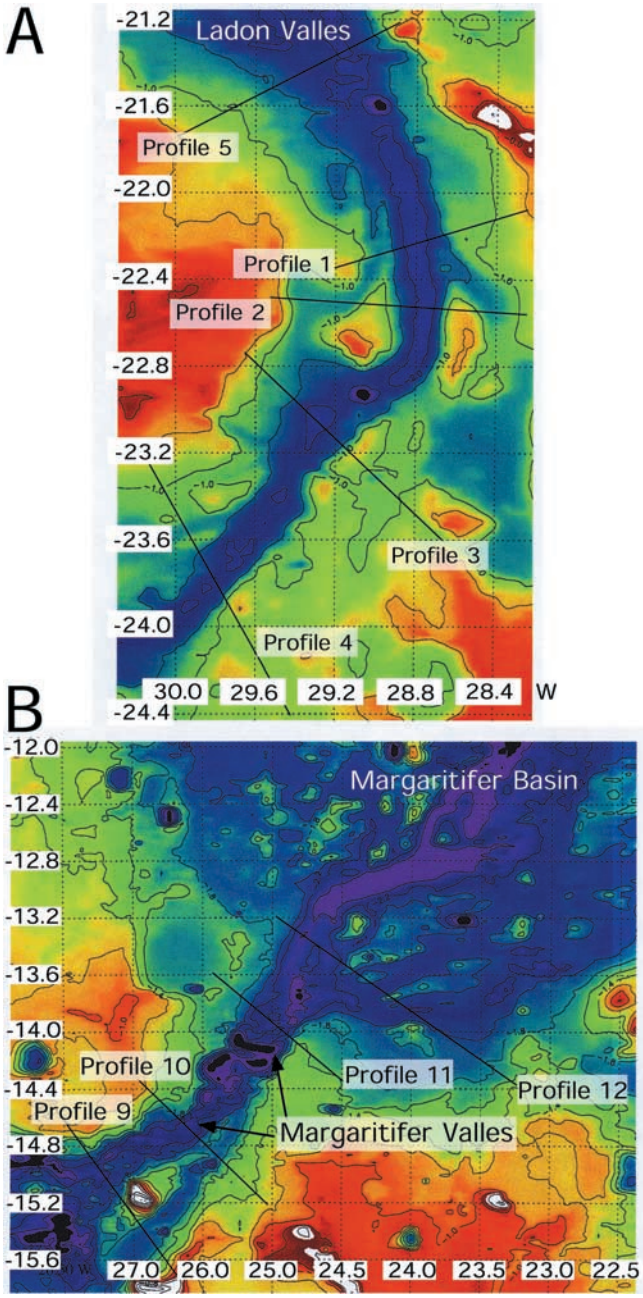

Figure 8. Gridded MOLA data (64 cells/degree) for (a) Ladon Valles and (b) Margaritifer Valles. Note the prominent central channel in both relative to terraces described in Figure 6, and the number of well-defined, terraced distributaries forming the distal reaches of Margaritifer Valles where it empties into Margaritifer Basin. Occurrence of the deeply incised central channels implies flow quickly coalesced leading to abandonment of the higher terraces. Locations of profiles used in estimation of discharge through the system (and listed in Table 1) are also identified. North is toward the top.

from the rim-breach at Uzboi Vallis (Figure 10b). These probable fan deposits are relatively flat-topped and fronted by slopes of ~3 degrees toward the crater interior. The fans are capped by linear to cuspate bed forms that are approximately 2 meters in height (based on 3 samples) and have a crest-to-crest spacing averaging 108 meters (based on 10 samples). The aspect ratio of the cuspate bed forms is dissimilar from that associated with most eolian dunes on Mars [e.g., *Malin et al.*, 1998], whereas their spacing versus height is broadly consistent with large scale current ripples on the Earth [*Allen*, 1968; *Baker and Nummedal*, 1978]. Superposition of small craters (Figure 10b) implies the cuspate bed forms are inactive and relatively ancient. On the basis of their association with the alluvial deposits, morphology, and apparent age, we suggest that the features are giant current ripples emplaced during late-stage discharge into crater Holden.

[24] A water-lain origin for the wedge-shaped deposits, associated cuspate bed forms, and layers in crater Holden places limits on the minimum depth and volume of water that ponded inside the crater. For example, the height and spacing of the cuspate features implies that deposition occurred in water at least tens of meters deep [*Baker and Nummedal*, 1978]. Hence, a first order estimate of the water depth in the crater is derived using the inferred water depth over the bed forms plus their elevation above the crater floor (Figure 11). MOLA data indicate the alluvial surfaces are at least 30 m above the crater floor and if at least 20 meters more water covered them at the time of deposition, then a minimum of 50 meters of water ponded inside the crater. This estimate is consistent with the depth inferred from the elevation at which layers form a bench against the crater wall.

[25] When multiplied by the area of the crater, a 50 m water depth translates to more than 750 km^3 of water. Although large, this volume represents the minimum late stage discharge into the crater because repeated episodes of inundation are likely required for forming the numerous layers and actual inundation depths may have been greater [e.g., *Parker*, 2000].

[26] The absence of an outlet from crater Holden indicates a lack of surface discharge associated with late stage flow and ponding. Subsurface discharge from the crater apparently did occur, however, and formed a small area of chaotic terrain northeast of the crater near Ladon Valles (Figure 11) [*Boothroyd*, 1983; *Parker*, 1985]. Formation of crater Holden would have fractured and disrupted preexisting coarsely bedded sediments in Holden Basin, thereby providing a ready pathway for subsurface drainage from the crater. MOLA data indicate the chaotic terrain is located at the lowest point around crater Holden (Figure 11). It is likely, therefore, that subsurface discharge from the crater initiated chaos formation as it drained into Ladon Valles [*Boothroyd*, 1983; *Parker*, 1985].

[27] Late stage discharge from Nirgal Vallis, ponding in crater Holden, and associated subsurface drainage and chaos formation marked the final stage of flow through the ULM system [*Parker*, 1985]. Evolution of the valley systems draining the eastern flank of the Chryse Trough was contemporaneous and is discussed next.

5. Samara and Parana-Loire Valles

5.1. Overview of Samara and Parana-Loire Valles

[28] Samara and Parana-Loire Valles (Figures 1 and 2) drain an area on the eastern flank of the Chryse trough

Table 1. Discharge Estimates for Ladon and Margaritifer Valles[a]

Ladon Valles Discharge Estimates								
Profile	Elevation	P to P Slope	D, m	n	V,[b] m s^{-1}	W, m	A, m^2	Q, m^3 s^{-1}
4	−2000	–	28	0.04	3.2	1,600	44,800	143,360
3	−2050	0.0009	256	Values not derived due to low confidence in depth estimate				
2	−2082	0.0005	500	Values not derived due to low confidence in depth estimate				
1	−2105	0.0014	88	0.04	6.7	6,400	563,200	3,773,440
5	−2010	Values suspect due to apparent deposition in mouth of channel, thus not used in calculations						
Margaritifer Valles Discharge Estimates								
Profile	Elevation	P to P Slope	D, m	n	V,[c] m s^{-1}	W, m	A, m^2	Q, m^3 s^{-1}
9	−2318	–	32	0.04	3.0	3,800	121,600	364,800
10	−2378	0.0014	78	0.04	5.3	3,900	304,200	1,612,260
11	−2375	0	25	0.04	2.5	5,300	132,500	331,250
12	−2400	0.0007	35	0.04	3.1	4,280	149,800	464,380

[a] Profile refers to profiles located in Figures 8 and 9. Elevation is MOLA derived elevation for thalweg of channel along profile. P to P Slope is indicated for that calculated between individual profiles. D, depth; n, Manning Roughness Coefficient; V, velocity; W, width; A, Area; Q, discharge.
[b] Used average slope of 0.0008 in mean velocity calculation.
[c] Used average slope of 0.0006 in mean velocity calculation.

roughly equivalent to 85% of the basin of the Colorado River before debouching into Margaritifer Basin at 14°S, 23°W. Like ULM, the location and orientation of valleys is significantly influenced by the multiringed basins [*Schultz et al.*, 1982; *Frey et al.*, 2001], and many are circumferential or radial to the basin centers.

5.2. Valley Morphometry

[29] Unlike the ULM system, Samara and Parana-Loire Valles are complete drainage networks, possessing collecting tributaries and well-defined stem or trunk valleys. Moreover, the valleys are mostly continuous, with only limited interruptions at depositional sinks. Evidence for a central channel within the valleys is largely absent, although MOC imagery is far from comprehensive. Nevertheless, medial Loire and Samara Valles present broad cross-sections and may preserve incipient floodplains. Confirmation of this statement is confounded by the modified nature of the surface as viewed in available MOC imagery: most local surfaces are peppered by small craters and variably buried by small dunes.

[30] Downcutting along medial Loire Vallis lowered the base level for adjacent tributaries that responded via increased stream power and incision. The distribution and deeply incised character of the tributaries that join medial Loire Vallis (Figure 1) are consistent with rapid entrenchment and headward extension of the tributaries under this scenario.

[31] As summarized from *Grant* [2000], preserved drainage densities in the Samara and Parana-Loire basins are among the highest on Mars [*Carr and Chuang*, 1997; *Grant*, 2000] at 0.03–0.11 km/km^2. Nevertheless, post-valley resurfacing (e.g., southwest of Parana Valles, Figure 5) destroyed some valley segments, thereby indicating original drainage densities were even higher. Basin ruggedness numbers (drainage density times total basin relief) are 0.005 to 0.086 and imply a fairly high flood potential for the drainages. Together with drainage density, these values suggest the systems evolved in substrates with fairly high infiltration and subsurface storage capacities [*Ritter et al.*, 1995].

[32] As described by *Pieri* [1980] and *Grant* [1987, 2000], the Margaritifer Sinus valleys are well integrated with limited internal drainage, but terrestrial relationships between various sinuosity parameters were not well expressed. While this is likely due in part to the networks' expression as valleys and not channels [*Grant*, 2000] it may also relate to a major role played by numerous impact craters in dictating stream course. Such control on valley course would be largely independent of the typical relationships between sediment load and transport capacity that strongly influence channel sinuosity on the Earth [*Ritter et al.*, 1995]. One location where crater-produced topography clearly controls drainage courses is along medial Samara Valles (29°S, 15°W) where a ~10 km diameter crater blocked the valley (Figure 12). Resultant upstream deposition extends for nearly 50 km and led to rerouting to the east around an ancient upland ridge before rejoining the original valley system ~250 km to the northwest.

[33] Most sub-basins associated with Samara and Parana-Loire Valles (Figure 2) are drained by fourth-order trunk valleys [after *Strahler*, 1952], possess tributaries that head near basin divides, and preserve a fairly even distribution of tributaries. The unit-less relief ratio for the basins (basin relief divided by basin length) is 0.0001–0.13 [*Grant*, 2000] and comparison with terrestrial relationships between relief ratio versus expected denudation rates [*Hadley and Schumm*, 1961; *Schumm*, 1963; *Gregory and Walling*, 1973; *Ritter et al.*, 1995] suggests erosion in Margaritifer Sinus was locally as high as ~1–2 meters per one thousand years if runoff was involved. In contrast to conclusions drawn by *Hynek and Phillips* [2001], however, preservation of heavily cratered surfaces and structures (e.g., relief associated with the multiringed impact basins) that continue to define the drainage basins and stream courses require that such high erosion rates were localized and geologically short-lived.

[34] Previous studies [e.g., *Malin and Carr*, 1999] have noted that Martian valley systems tend to be scale dependent and separated by largely undissected interfluves. In addition, *Grant* [2000] noted minimal down-valley variation in width and cross-section in Margaritifer Sinus, thereby implying little downstream increase in discharge. Some tributaries to Samara Valles, however, are not only scale independent, but also vary significantly in width

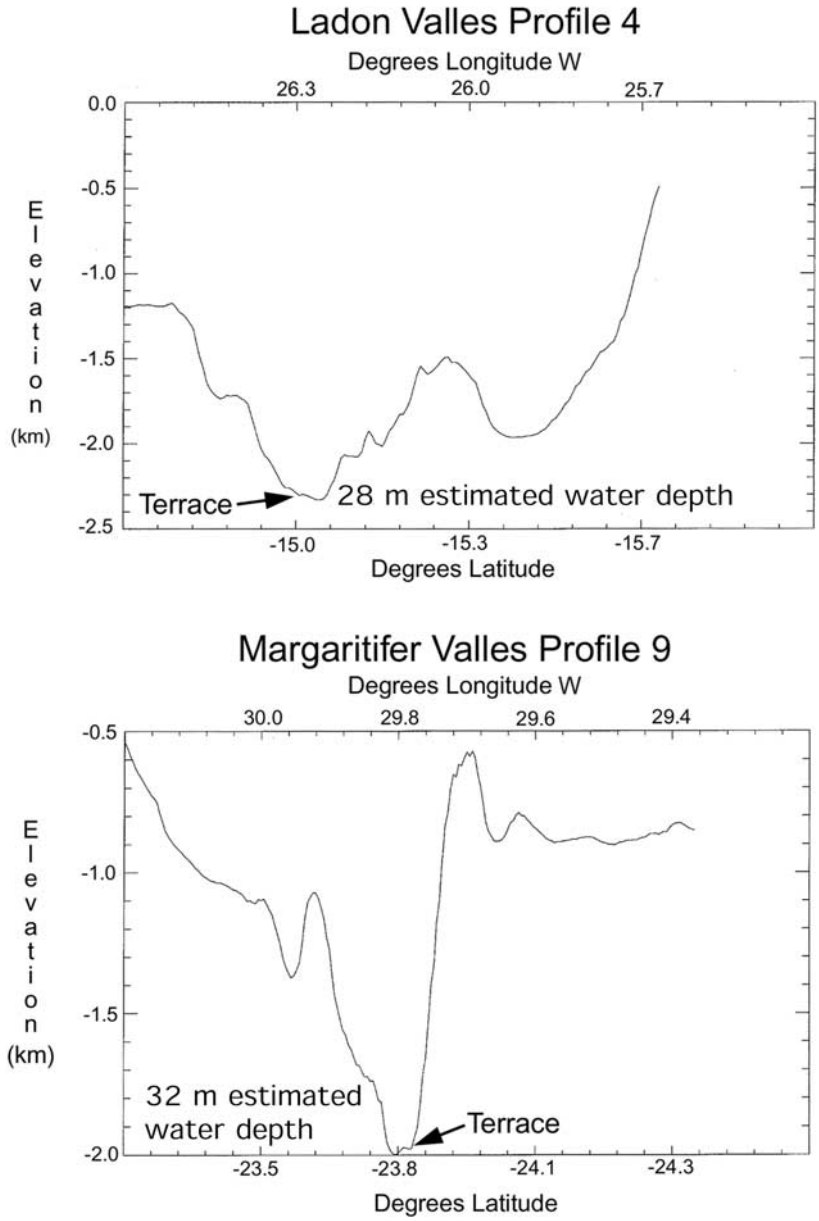

Figure 9. Examples of MOLA profiles across Ladon Valles (top) and Margaritifer Valles (bottom) showing terraces selected for use in estimating flow depths and channel cross sections. Profile numbers correspond to those identified in Figure 8.

downstream (Figure 13). These tributaries surround and drain an isolated ridge near 31.5°S, 9°W that lacks any obvious source for discharge (Figure 13). The tributaries decrease in scale and order toward the ridge crest in a manner reminiscent of runoff-induced rilling and incisement on terrestrial hillslopes, albeit at a much larger scale. In some instances, the tributaries can be traced to within a few hundreds of meters of the ridge crest (Figure 13).

[35] On the Earth, channel initiation requires runoff with sufficient tractive force to entrain sediment and begin incisement [e.g., *Ritter et al.*, 1995]. Typically, there is some critical distance from the divide where incisement does not occur because slope and/or depth of overland flow imparts insufficient shear across the bed to initiate transport. Although MOC image resolution does not permit assessing whether the Samara Valles tributaries exhibit these relationships at the small scale, their locally scale independent nature and tendency to head very close to the ridge crest presents an intriguing similarity.

[36] The Samara tributaries also possess a down-valley longitudinal profile similar to that observed along terrestrial systems formed by runoff (Figure 14). Slope is a principal adjusting factor in terrestrial drainages and responds to changing sediment size and load [*Ritter et al.*, 1995].

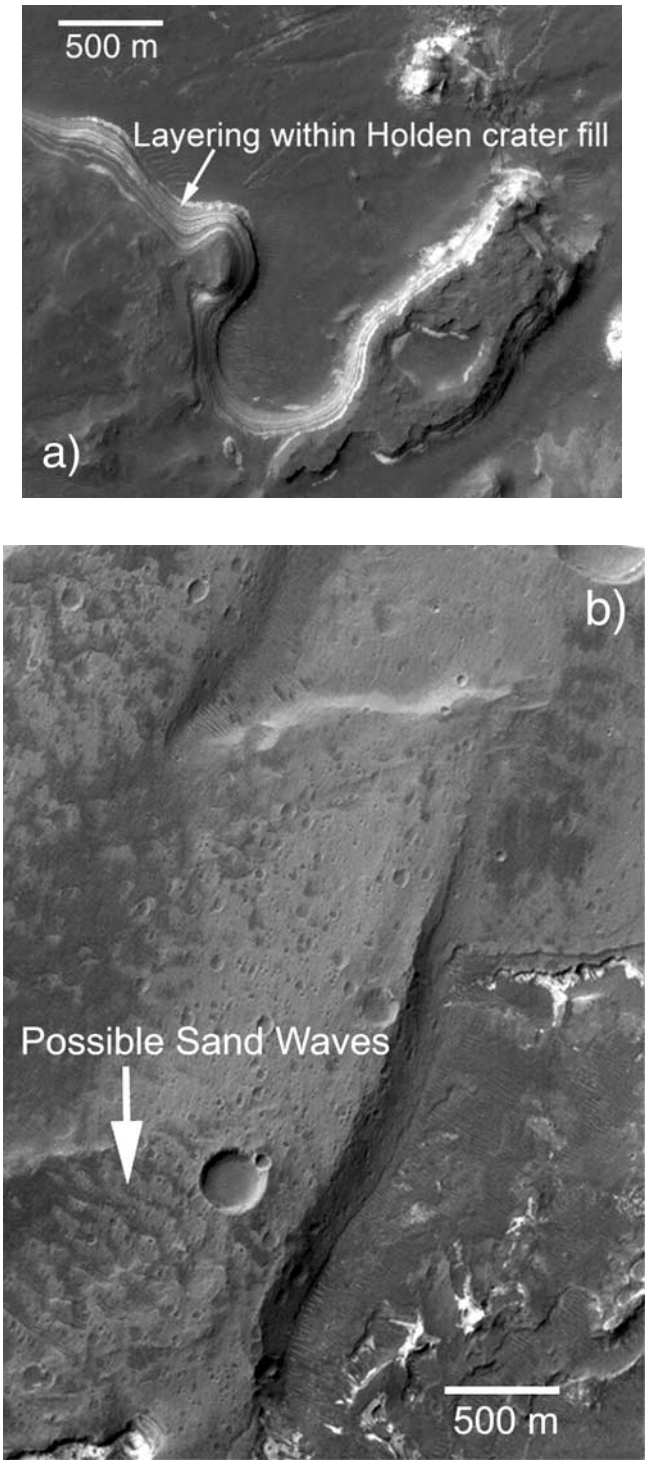

Figure 10. Layering in sediments on the floor of Holden Crater (a) and possible sand wave bed forms deposited on alluvium where Uzboi Vallis discharged into the crater (b). Note the layers in (a) are thin (to the limit of the image resolution) and continuous over distances of kilometers, consistent with emplacement in standing water. Similarly, the bed forms in (b) are comparable in height and spacing to giant ripples formed in the Channeled Scablands, but differ in aspect ratio from that associated with typical eolian dunes formed on Mars. Both images are subsets of MOC image M0302733, centered at 27.1°S, 34.9°W, with 2.8 m/pixel resolution. North is toward the top of both (a) and (b).

Correspondingly, terrestrial systems in dynamic equilibrium display a concave up longitudinal profile as a reflection of the generally decreasing grain size and necessary stream power for transport with increasing downstream distance [*Ritter et al.*, 1995]. The longitudinal profiles of the Samara tributaries are not diagnostic of an origin related to overland flow, but the attribute does suggest increasing discharge and decreasing transported grain size in the downstream direction [*Ritter et al.*, 1995]. If verified, this property would contradict inferences drawn from examination of other tributaries (e.g., Parana Valles) that possess a constant valley width, cross-section, and implied downstream discharge.

5.3. Deposition Associated With Samara and Parana-Loire Valles

[37] In general, deposits associated with Samara and Parana-Loire Valles are limited to several impact craters and Parana Basin (Figures 1 and 2). Exceptions include the isolated impact blockage of Samara Valles and possible storage of some sediment along incipient floodplains. There is no recognizable evidence for deposition at the mouth of the systems.

[38] Three of the largest crater-filling basins along the valleys include the Clota-Oltis craters (24.5°S, 20.5°W and 23.0°S, 20.5°W), S2 (27.5°S, 18.5°W), and Parana Basin (22.5°S, 12.5°W). Each of these crater-basins contains significant sediment relative to the volume associated with incisement of upstream valley segments [*Grant*, 2000].

[39] The volume of fill within each basin was calculated using the initial crater volume minus the volume remaining unfilled [*Grant*, 2000], where initial crater volume is based on depth/diameter estimates [*Pike*, 1981; *Garvin and Frawley*, 1998] and the volume remaining unfilled was derived using MOLA data and/or shadow measurements. Depth of infilling was corroborated in Parana Basin based on the thickness required for near burial of intrabasin craters. Viking and MOC data (where available) indicate only minor contributions due to infilling by non-fluvial processes (few 10s of meters at most), suggesting that derived sediment volumes approximate alluvial infilling. Hence, the estimated alluvium volume in the sinks is 5,000 km^3, 5,300 km^3, and 23,300 km^3 for the Clota-Oltis, S2, and Parana basins, respectively [*Grant*, 2000].

[40] The volume of sediment represented by excavation of valleys upstream of the crater-basins was estimated [*Grant*, 2000] using measured valley widths and lengths, assuming both triangular and trapezoidal cross sections [*Goldspiel and Squyres*, 1991], and a drainage density of 0.07 km/km^2 (derived for the well-preserved Parana Valles) to compensate for possible destroyed valley segments. Resultant volume estimates for the excavated valleys are 3,000 km^3, 2,900 km^3, and 14,200 km^3 for the Clota-Oltis, S2, and Parana basins, respectively [*Grant*, 2000].

[41] In all cases, the volume represented by excavation of valley segments upstream of the basins is less than 60% of the alluvium volume (assuming uniform bulk densities, see [*Grant and Schultz*, 1993a; *Grant*, 2000]). Although these estimates incorporate uncertainty related to measured drainage density, non-alluvial basin infilling, and valley cross-section, such parameters are second-order and cannot account for the differences in volume estimates. Moreover,

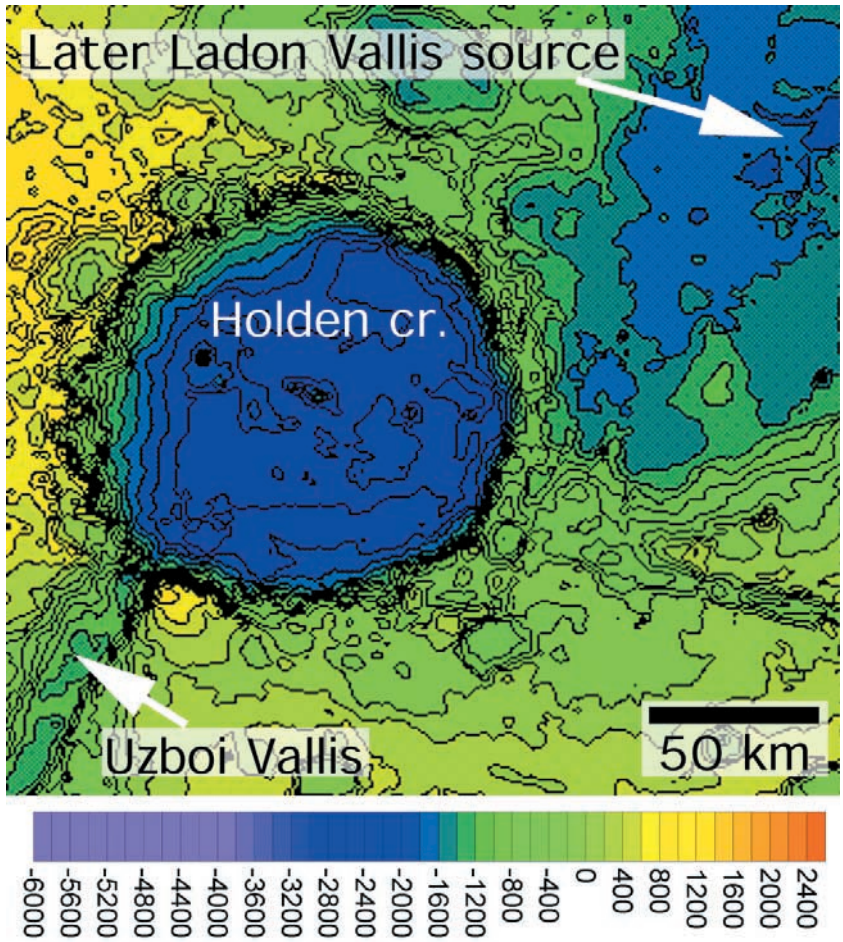

Figure 11. Gridded MOLA data (64 cells/degree, 200 m interval) of the ~140 km diameter Holden crater (centered at approximately 26.0°S, 34.2°W). The crater floor is fairly flat over horizontal distances exceeding 100 km, consistent with relief associated with lacustrine deposition. The late stage source for Ladon Vallis appears in the northeast corner of Holden basin. The image is bounded by 23.6°S, 28.4°S, 31°W, and 36°W.

estimates for the sinks do not include any additional transported sediment that may be stored in incipient floodplains, or associated with local damming (e.g., medial Samara Valles). The comparative volume estimates suggest that valley excavation alone cannot account for all alluvium in the sinks and that transport of additional sediment from upstream basin surfaces via overland flow was involved. Point-source discharge along the valleys by groundwater sapping cannot account for the total alluvium inventory.

6. A Model for Martian Valley Formation

[42] The range of morphometric data for the Margaritifer Sinus valleys paints a contradictory picture with respect to processes responsible for their formation. For example, low drainage densities, ruggedness numbers, generally uniform valley widths and cross-sections, scale dependence, and paucity of incised interfluves are consistent with formation by groundwater sapping. By contrast, the basin-wide distribution of valleys, degree of integration, minimal internal drainage, tendency to head near basin divides, excess alluvium in sinks, and character of some tributaries favors an origin by surface runoff. Although none of the morphometric parameters provides conclusive evidence for valley formation by sapping versus runoff, as a suite they are consistent with a model involving both processes.

[43] Valley incisement dominated by precipitation recharged groundwater sapping and limited runoff is consistent with the characteristics described here and by others [e.g., *Malin and Carr*, 1999; *Grant*, 2000]. Valley morphometry implies limited runoff from highly permeable substrates possessing high infiltration and storage capacity. Hence, most precipitation would directly enter the subsurface with lateral deflection and discharge along layers/aquitards. Basin-wide recharge via precipitation satisfies the requirement that valleys are widely distributed and typically head near divides. Moreover, the scale dependence of most valleys and generally undissected interfluves (Figure 12) are consistent with a paucity of runoff during all but the most extreme precipitation events [*Grant and Schultz*, 1994].

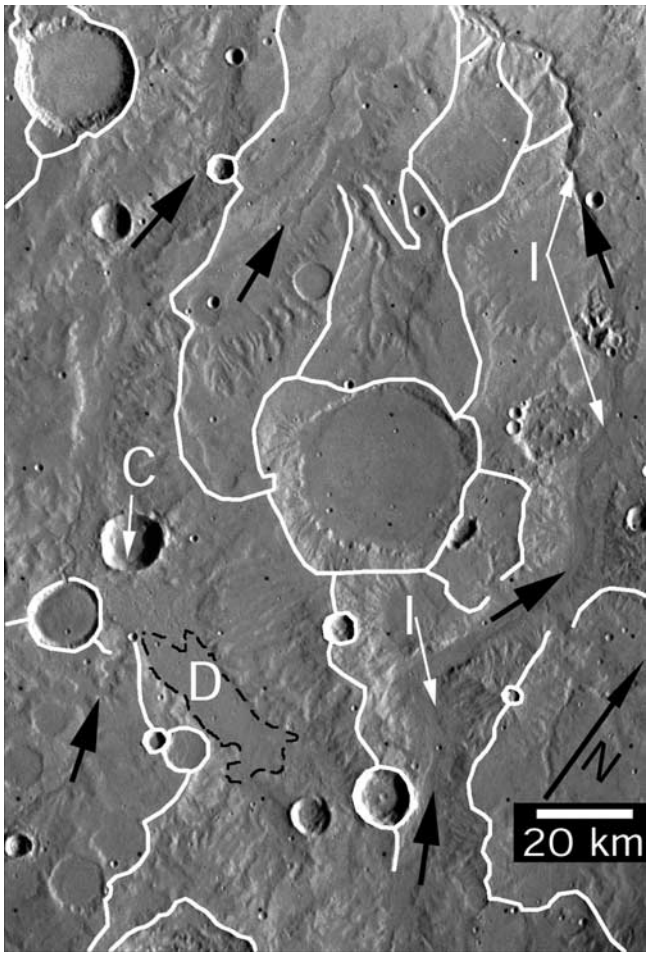

Figure 12. Viking Orbiter image of medial Samara Valles where it incises a broad ridge of ancient highlands material. Drainage was initially along the left side of the image, but this was interrupted by the formation of a crater (marked C) and emplacement of associated ejecta. The blockage resulted in upstream deposition (marked D) and diversion of Samara Valles to the east where a new, deeper valley (marked I) was incised. Flow eventually rejoined the original valley ~250 km to the northwest. Black arrows denote flow direction and white lines mark drainage divides as defined by stereo mapping. This is part of Viking image 084a41, centered at 28.3°S, 15.8°W. The image is ~130 km across.

[44] In this model, valley morphometry consistent with sapping would be exaggerated, especially following cessation of precipitation and final draw down of aquifers. Nevertheless, basin-wide characteristics and isolated locations possessing less permeable substrates would evolve signatures of runoff (e.g., the Samara Valles tributaries, Figure 13). Infrequent high magnitude precipitation would exceed surface infiltration capacities and lead to runoff and transport of sediment that can account for excess alluvium in sinks.

[45] Evolving drainage networks on the continuous ejecta surrounding Meteor Crater in Arizona may be good analogs for Martian valleys. Hydraulic conductivity and infiltration rates derived for the ejecta average 7–8 meters/day and 7–

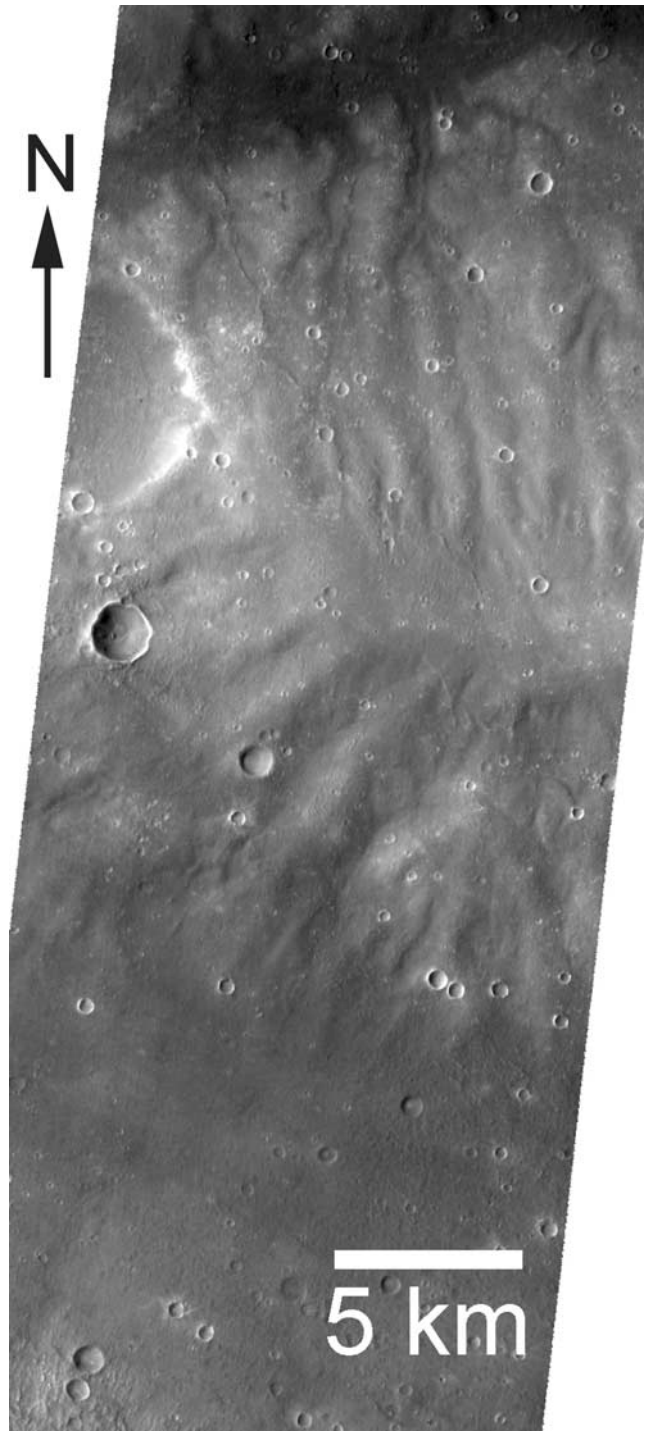

Figure 13. Samara Valles tributaries that head near a local east-west divide running through the center of MOC image AB107706, centered at 32.0°S, 9.15°W, with 15.4 m/pixel resolution. The distribution of the tributaries relative to the ridge crest is similar to the character expected for drainages created by runoff. A critical distance may separate the unincised region adjacent to the drainage divide from locations where runoff impinged sufficient shear stress to initiate incisement. Note that the valleys display central sinuous ridges that frequently extend from the trunk Samara Valles to near the divide. These ridges could be coarse channel deposits now expressed as positive relief due to subsequent deflation of adjacent, finer grained surfaces.

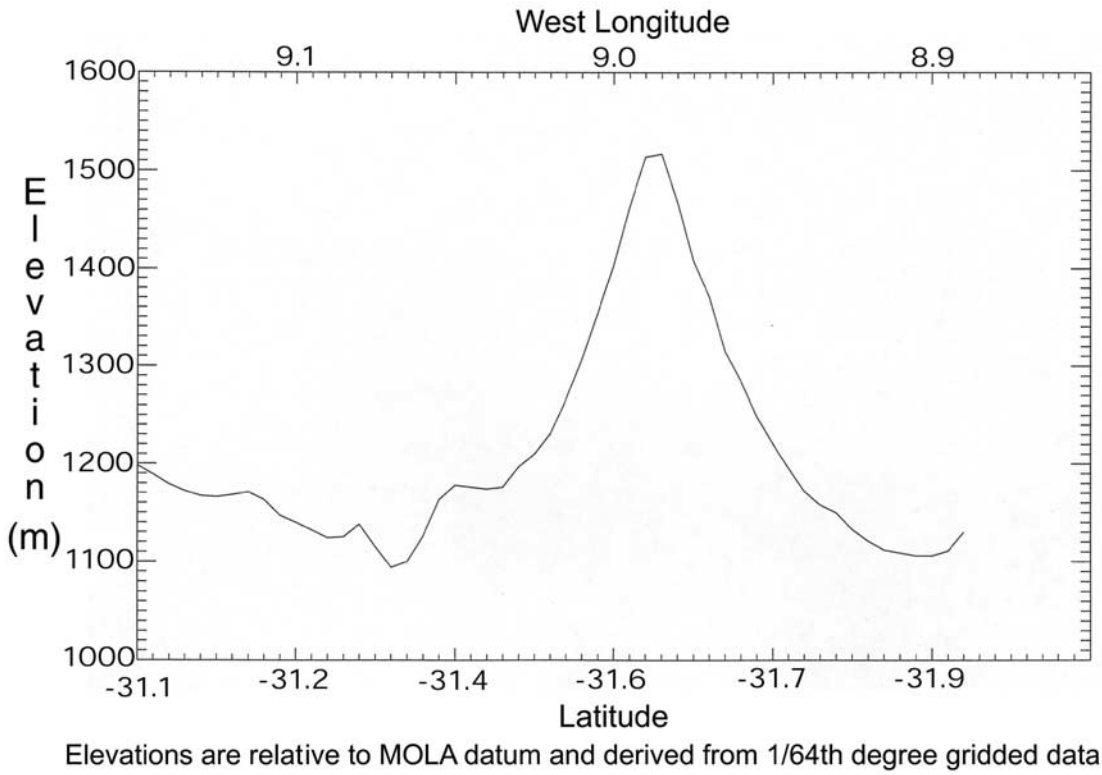

Figure 14. MOLA profile from north to south across ridge incised by Samara Valles tributaries shown in Figure 13 (profile crosses ridge very near and approximately parallel to the right edge of Figure 13). Note the concave-up character of the profile on the ridge flanks, a characteristic commonly evolved on terrestrial slopes being eroded by runoff.

10 cm/hour, respectively [*Grant and Schultz*, 1993b, 1994], thereby requiring significant rainfall to produce runoff on the ejecta. For example, ~3 cm of rainfall in a 24 hour period comprises the one year precipitation event at Meteor Crater [*Miller et al.*, 1977], but results in little runoff. By contrast, surrounding in situ surfaces and the steep crater walls experience significant runoff for the same event [*Grant and Schultz*, 1993b].

[46] Incisement in and around Meteor Crater mirrors the relative importance of infiltration versus runoff and leads to contrasting drainage expression on crater walls versus the continuous ejecta [*Grant*, 1999]. On crater walls, high gradients and minimal infiltration maximize runoff and stream power causing rapid incisement of debris chutes. On the ejecta, lesser gradients, higher infiltration, and limited stream power enable a network of small radial systems near the upper rim that deposit coalescing fans along the lower flank. Drainage densities inside and outside the crater reflect the contrasting settings and are 13.7 km/km^2 and 3.4 km/km^2, respectively (derived from same-scale air-photos).

[47] On Mars, impacts have created a regolith [e.g., *Carr*, 1996] of mixed ejecta deposits and fragmented bedrock that is punctuated by competent layers [*Malin et al.*, 1998]. By analogy to Meteor Crater, Martian regolith may possess high infiltration capacities and hydraulic conductivities. Hence, initiating runoff from most surfaces likely requires significant precipitation. A resultant predominance of sapping is consistent with most Mars valley morphology (e.g., invariant down valley width, mostly undissected interfluves), but valley morphometry also reflects the role of precipitation in basin wide recharge of aquifers and accounts for uniform valley distribution and good integration. Less permeable and/or steeper surfaces would experience more runoff during precipitation, thereby accounting for disparate drainage densities and scale independence on some crater walls and ridges (Figure 13).

[48] Either rainfall or melting snow could provide the water for valley formation in the proposed model: both would distribute recharge across drainage basins for concentration via infiltration and interflow along aquitards. Although average rainfall events could have been small, occasionally larger events (or a higher frequency of events) would be required for runoff. Alternatively, if snowfall were responsible for recharge, the necessity for precipitation of higher magnitude or frequency is relaxed because melting of an accumulated snowpack could overwhelm surface infiltration capacities.

[49] Widespread air fall deposits characterized by abundant volatiles have been postulated for Mars and provide a potential source of water for valley formation. Air fall deposits occur in the Electris region, northwest of Isidis, southern Ismenius Lacus, and Isidis Basin [*Grizzaffi and*

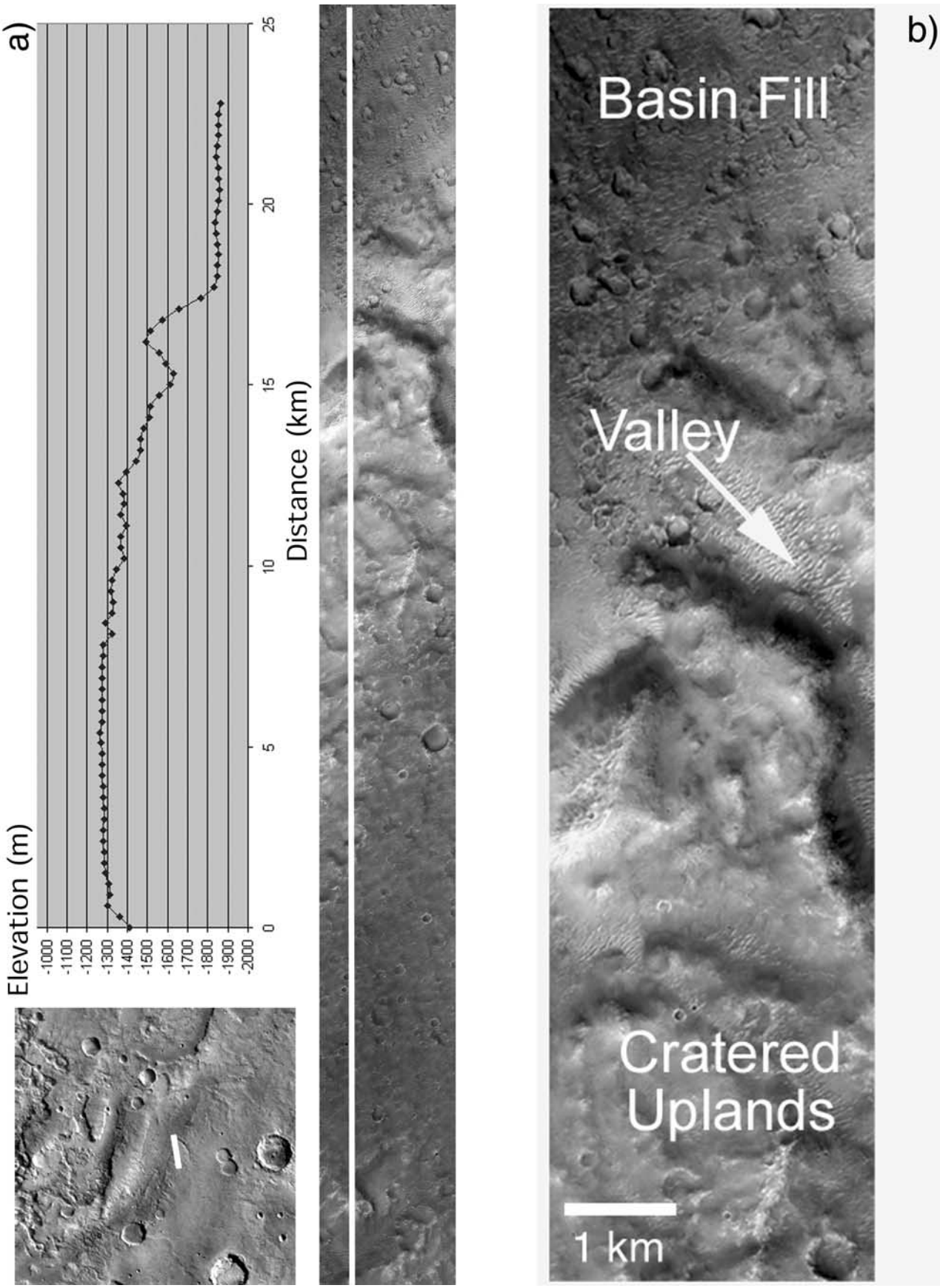
a)
Elevation (m)
-1000
-1100
-1200
-1300
-1400
-1500
-1600
-1700
-1800
-1900
-2000
0
5
10
15
20
25
Distance (km)
b)
Basin Fill
Valley
Cratered
Uplands
1 km

Schultz, 1989; *Grant and Schultz*, 1990, 1993a]. Their emplacement coincided with increased geomorphic activity in Sinus Meridiani, the vicinity of crater Millochau, and elsewhere [*Schultz and Lutz*, 1988; *Grant and Schultz*, 1993a] and was approximately concurrent with valley formation in Margaritifer Sinus. Partial preservation of the deposits and their wide distribution argues for a global epoch of increased gradation, consistent with an active water cycle that included precipitation, recharge of aquifers, and valley formation.

7. Evidence for Extensive Ponding in Margaritifer Basin

[50] Discharge from the ULM into Margaritifer Basin (Figures 1 and 3) was via a complex series of distributaries at varying, but generally lower elevations than the Samara and Parana-Loire Valles outlet. The ULM distributaries appear to truncate the Samara and Parana-Loire outlet suggesting ULM discharge post-dated that from Samara and Parana-Loire. The number and scale of erosional remnants and distributary channel segments associated with Margaritifer Valles indicates that the volume of water effusing from the ULM system was dominant.

[51] The distribution of upland remnants and the ULM distributaries further implies ponding within Margaritifer Basin occurred in northward-expanding stages. Initial discharge apparently caused considerable localized ponding near the mouths of the ULM, Samara, and Parana-Loire Valles. An increasing depth of ponding, however, resulted in overtopping of a broad ridge oriented NW to SE (at 6°S, 23°W to 10°S, 17°W, see Figure 3) at −1.5 km elevation (MOLA datum) and ponding farther north and east. Breaching of the ridge occurred in at least three separate locations (Figure 3), with flow becoming concentrated in the westernmost channel as evidenced by the substantially greater depth of incisement. Sediments deposited during early discharge into Margaritifer Basin were eroded when breaching of the ridge lowered the base level. As deposition shifted northeast to the vicinity of 2°S, 16°W (Figures 3 and 8b), older terraced distributaries associated with initial ponding were abandoned.

[52] Fill within Margaritifer Basin is uniform in texture, has low relief, and lies at an elevation of approximately −1.9 km (Figures 15a and 15b). Both MOC and Viking imagery of the basin deposits reveal an absence of lobate structures or morphology (e.g., possible tumuli, leveed channels, sinuous channels) that might suggest a non-fluvial mode of emplacement.

[53] While the extent of ponding in Margaritifer Basin remains uncertain, it reached at least to Margaritifer Chaos, the head of Ares Valles, and Sinus Meridiani (Figure 3) and perhaps beyond (Figures 15a and 15b). For example, *Edgett and Parker* [1997] suggested that deposits at approximately the same elevation in nearby Sinus Meridiani were due to deposition into standing water and may be related.

8. Fate of the Water

[54] The ultimate sink for water from the ULM and Samara and Parana-Loire valley systems is unknown, but ponding in Margaritifer Basin must have resulted in infiltration and subsurface water storage. Much of the basin is between the third and fourth rings of Ladon Basin and is likely characterized by a thick layer of brecciated, fractured basin ejecta [*Schultz et al.*, 1982]. Moreover, Margaritifer Basin overlies the rings of Ladon and Chryse Basins [*Shultz and Glicken*, 1979; *Schultz et al.*, 1982] and several smaller basins [*Frey et al.*, 2001]. The combination of thick regolith and fractures would have created a zone of increased permeability and structural weakness [*Grant*, 1987], thereby enabling subsurface water storage.

[55] Crater statistics confirm that formation of Margaritifer and Iani Chaos began shortly after cessation of channel and valley formation in the early to mid Hesperian and provided water for incisement of Ares Vallis (Figures 3 and 4) [see *Carr*, 1979; *Carr and Clow*, 1981; *Rotto and Tanaka*, 1995]. As first proposed by *Carr* [1979], surface collapse and release of water associated with chaos formation may have been triggered when deteriorating climate led to development of a thickening layer of permafrost. Thickening permafrost would have confined the aquifer, causing increasing hydrostatic pressure, and leading to rupture, discharge, and surface collapse. The geologic setting of Margaritifer Basin would have been predisposed to chaos formation following valley and channel formation.

[56] Although Margaritifer and Iani Chaos formation began shortly after discharge from ULM and the Samara and Parana/Loire systems ended [*Rotto and Tanaka*, 1995], the bulk of collapse and discharge likely occurred later [*Masursky et al.*, 1977; *Carr*, 1979; *Rotto and Tanaka*, 1995]. Ongoing collapse suggests that water was released in pulses over an extended period, consistent with a model for chaos formation [*Carr*, 1979] where water release relieves hydrostatic pressure, stabilizes the surface, and reinitiates the process.

9. Conclusions

[57] The Margaritifer Sinus region records a long and complex drainage history. Drainage across western sections was dominated by the segmented ULM system that heads south of Argyre Basin. By contrast, eastern surfaces are incised by the well-integrated and high density Samara and Parana-Loire Valles. Valley morphometry supports an origin related to precipitation-recharged groundwater sapping.

Figure 15. (opposite) (a) Transition from cratered upland (lower half of image) to floor of Margaritifer Basin (upper quarter), in MOC image M0801461 (centered at 8.7°S, 17.7°W, 2.87 km across, 15.4 m/pixel resolution). The corresponding MOLA topographic profile (white line on image) is shown in the upper left, and the regional Viking context image is shown at lower left. The floor of Margaritifer Basin has very low relief, is devoid of flow fronts or other features, and associated materials embay valley networks. (b) Enlarged subset of this image. Characteristics of the basin fill are consistent with alluvial/lacustrine deposition. North is toward the top.

[58] Both the ULM and valley systems formed from late Noachian into the early Hesperian, but discharge from ULM was greatest and probably rivaled that of the Channeled Scabland on the Earth. Channel and valley evolution in Margaritifer Sinus approximately coincides with enhanced geomorphic activity elsewhere on Mars.

[59] All the channel and valley systems discharged into Margaritifer Basin along the axis of the Chryse Trough and caused ponding that reached northward at least to Margaritifer and Iani Chaos and the head of Ares Vallis. Margaritifer Basin is located between the outer rings of Ladon and Chryse basins and is likely underlain by a thick deposit of ejecta. Consequently, water ponded in Margaritifer Basin infiltrated and was stored in the subsurface. Subsequent release of this water in the middle Hesperian carved the northward-draining Ares Vallis.

[60] **Acknowledgments.** Thanks to Herb Frey for providing access to MOLA data, Scott Anderson for generating MOC/MOLA data, and Ross Irwin for formatting and improving the figures. We appreciate comments from Bruce Campbell, Cathy Weitz, and an anonymous reviewer.

References

Allen, J. R. L., *Current Ripples and Their Relation to Patterns of Water and Sediment Motion*, 433 pp., Elsevier Sci., New York, 1968.

Baker, V. R., *The Channels of Mars*, 198 pp., Univ. of Tex. Press, Austin, 1982.

Baker, V. R., and D. Nummedal, *The Channeled Scabland: A Guide to the Geomorphology of the Columbia Basin, Washington: Prepared for the Comparative Planetary Geology Field Conference Held in the Columbia Basin June 5–8, 1978*, 186 pp., NASA, Washington, D. C., 1978.

Baker, V. R., M. H. Carr, V. C. Gulick, C. R. Williams, and M. S. Marley, Channels and valley networks, in *Mars*, edited by H. H. Kieffer et al., pp. 493–522, Univ. of Ariz. Press, Tucson, 1992.

Banerdt, W. B., Surface drainage patterns on Mars from MOLA topography, *Eos Trans. AGU*, *81*(48), Fall Meet. Suppl., P52C-04, 2000.

Boothroyd, J. C., Fluvial drainage systems in the Ladon Basin area: Margaritifer Sinus area, *Mars, Geol. Soc. Am. Abstr. Programs*, *15*, 530, 1983.

Carr, M. H., Formation of Martian flood features by the release of water from confined aquifers, *J. Geophys. Res.*, *84*, 2995–3007, 1979.

Carr, M. H., *The Surface of Mars*, 232 pp., Yale Univ. Press, New Haven, Conn., 1981.

Carr, M. H., *Water on Mars*, 229 pp., Oxford Univ. Press, New York, 1996.

Carr, M. H., and F. C. Chuang, Martian drainage densities, *J. Geophys. Res.*, *102*, 9145–9152, 1997.

Carr, M. H., and G. D. Clow, Martian channels and valleys: Their characteristics, distribution and age, *Icarus*, *48*, 91–117, 1981.

Craddock, R. A., and K. L. Tanaka, Estimates of the maximum and minimum flow velocities of the circum-Chryse outflow channels, in *Mars Pathfinder Landing Site Workshop II*, edited by M. P. Golombek et al., *LPI Tech. Rep. 95-01*, pp. 9–10, Lunar and Planet. Inst., Houston, Tex., 1995.

Edgett, K. S., and T. J. Parker, Water on early Mars: Possible subaqueous sedimentary deposits covering ancient cratered terrain in western Arabia and Sinus Meridiani, *Geophys. Res. Lett.*, *24*, 2897–2900, 1997.

Ford, J. P., J. J. Plaut, C. M. Weitz, T. G. Farr, D. A. Senske, E. R. Stofan, G. Michaels, and T. J. Parker, *Guide to Magellan Image Interpretation, JPL Publ. 93-24*, NASA, Washington, D. C., 1993.

Frey, H. V., K. M. Shockey, E. L. Frey, J. H. Roark, and S. E. H. Sakimoto, A very large population of likely buried impact basins in the northern lowlands of Mars revealed by MOLA data, *Lunar Planet. Sci.*, *XXXII*, 1680, 2001.

Garvin, J. B., and J. J. Frawley, Geometric properties of Martian impact craters: Preliminary results from the Mars Orbiter Laser Altimeter, *Geophys. Res. Lett.*, *25*, 4405–4408, 1998.

Goldspiel, J. M., and S. W. Squyres, Ancient aqueous sedimentation on Mars, *Icarus*, *89*, 392–410, 1991.

Grant, J. A., The geomorphic evolution of Eastern Margaritifer Sinus, Mars, in *Advances in Planetary Geology, NASA Tech. Memo.*, *89871*, 1–268, 1987.

Grant, J. A., Evaluating the evolution of process specific degradation around impact craters, *Int. J. Impact Eng.*, *23*, 331–340, 1999.

Grant, J. A., Valley formation in Margaritifer Sinus, Mars, by precipitation-recharged ground-water sapping, *Geology*, *28*, 223–226, 2000.

Grant, J. A., and T. J. Parker, The history of water discharge in the Margaritifer Sinus region, Mars, *Geol. Soc. Am. Abstr. Programs*, *32*, A303, 2000.

Grant, J. A., and T. J. Parker, The history of water discharge in the Margaritifer Sinus region of Mars, *Lunar. Planet. Sci.*, *XXXII*, 1224, 2001.

Grant, J. A., and P. H. Schultz, Gradational epochs on Mars: Evidence from west-northwest of Isidis Basin and Electris, *Icarus*, *84*, 166–195, 1990.

Grant, J. A., and P. H. Schultz, Degradation of selected terrestrial and Martian impact craters, *J. Geophys. Res.*, *98*, 11,025–11,042, 1993a.

Grant, J. A., and P. H. Schultz, Erosion of ejecta at Meteor Crater, Arizona, *J. Geophys. Res.*, *98*, 15,033–15,047, 1993b.

Grant, J. A., and P. H. Schultz, Early fluvial degradation in Terra Tyrrhena, Mars: Constraints from styles of crater degradation on the Earth, *Proc. Lunar Planet. Sci. Conf. 25th*, 457–458, 1994.

Gregory, K. J., and D. E. Walling, *Drainage Basin Form and Process*, 456 pp., Edward Arnold, London, 1973.

Grizzaffi, P., and P. H. Schultz, Isidis Basin: Site of ancient volatile-rich debris layer, *Icarus*, *77*, 358–381, 1989.

Hadley, R. F., and S. A. Schumm, Sediment sources and drainage basin characteristics in upper Cheyenne River basin, *U.S. Geol. Surv. Water Supply Pap.*, *1531-B*, 137–196, 1961.

Hodges, C. A., Geologic map of the Argyre quadrangle of Mars, scale 1:5M, *U.S. Geol. Surv. Misc. Invest. Ser., Map I-1181*, 1980.

Hynek, B. M., and R. J. Phillips, Evidence for extensive denudation of the Martian highlands, *Geology*, *29*, 407–410, 2001.

Komar, P. D., Comparisons of the hydraulics of water flows in Martian outflow channels with flows of similar scale on Earth, *Icarus*, *37*, 156–181, 1979.

Malin, M. C., and M. H. Carr, Ground-water formation of Martian valleys, *Nature*, *397*, 589–591, 1999.

Malin, M. C., and K. S. Edgett, Sedimentary rocks of early Mars, *Science*, *290*, 1927–1937, 2000.

Malin, M. C., et al., Early views of the Martian surface from the Mars Orbiter Camera of Mars Global Surveyor, *Science*, *279*, 1681–1685, 1998.

Mars Channel Working Group, Channels and valleys on Mars, *Geol. Soc. Am. Bull.*, *94*, 1035–1054, 1983.

Masursky, H., J. M. Boyce, A. L. Dial, G. G. Schaber, and M. E. Strobell, Classification and time of formation of Martian channels based on Viking data, *J. Geophys. Res.*, *82*, 4016–4038, 1977.

Miller, A. E., R. H. Fredrick, and R. J. Tracey, *Precipitation Frequency Atlas of the Western U.S., NOAA Atlas 2*, U.S. Dep. of Commerce, Washington, D. C., 1977.

Parker, T. J., Geomorphology and geology of the southwestern Margaritifer Sinus-Northern Argyre region of Mars, Master's thesis, Calif. State Univ., Los Angeles, 1985.

Parker, T. J., Martian paleolakes and oceans, Ph.D. thesis, Univ. of Southern Calif., Los Angeles, 1994.

Parker, T. J., A brief summary of the geomorphic evidence for an active surface hydrologic cycle in Mars' past, in *2nd International Conference on Mars Polar Science and Exploration*, pp. 142–143, *LPI Contrib. 1057*, Lunar Planet. Inst., Houston, Tex., 2000.

Phillips, R. J., M. A. Bullock, D. H. Grinspoon, B. M. Hynek, O. Aharonson, R. M. Williams, and S. A. Hauck, Did Tharsis influence climate and fluvial activity on Mars?, *Eos Trans. AGU*, *81*(48), Fall Meet. Suppl., P52C-02, 2000.

Phillips, R. J., M. T. Zuber, S. C. Solomon, M. P. Golombek, B. M. Jakosky, W. B. Banerdt, R. M. E. Williams, B. M. Hynek, O. Aharonson, and S. A. Hauck II, Ancient geodynamics and global-scale hydrology on Mars, *Science*, *291*, 2587–2591, 2001.

Pieri, D. C., Martian valleys: Morphology, distributions, age, and origin, *Science*, *210*, 895–897, 1980.

Pike, R. J., Crater depths on Mars: New data from Viking photogrammetry, *Proc. Lunar Planet. Sci. Conf. 12th*, 839–841, 1981.

Ritter, D. F., R. C. Kochel, and J. R. Miller, *Process Geomorphology*, 540 pp., Wm. C. Brown, Dubuque, Iowa, 1995.

Rotto, S., and K. L. Tanaka, Geologic/Geomorphic map of the Chryse Planitia region of Mars, scale 1:5M, *U.S. Geol. Surv. Misc. Invest. Ser., Map I-2441*, 1995.

Saunders, S. R., Geologic map of the Margaritifer Sinus Quadrangle of Mars, scale 1:5M, *U.S. Geol. Surv. Map I-1144*, MC-19, 1979.

Schultz, P. H., and H. Glicken, Impact crater and basin control of igneous processes on Mars, *J. Geophys. Res.*, *84*, 8033–8047, 1979.

Schultz, P. H., and F. E. Ingerson, Martian lineaments from Mariner 6 and 7 images, *J. Geophys. Res.*, *78*, 8415–8427, 1973.

Schultz, P. H., and A. B. Lutz, Polar wandering of Mars, *Icarus*, *73*, 91–141, 1988.

Schultz, P. H., R. A. Schultz, and J. Rogers, The structure and evolution of ancient impact basins on Mars, *J. Geophys. Res.*, *87*, 9803–9820, 1982.

Schumm, S. A., Disparity between present rates of denudation and orogeny, *U.S. Geol. Surv. Prof. Pap.*, *454-H*, 1963.
Scott, D. H., and K. L. Tanaka, Geologic map of the Western Equatorial Region of Mars, scale 1:15M, *U.S. Geol. Surv. Misc. Invest. Ser., Map I-1802-A*, 1986.
Smith, D. E., et al., The global topography of Mars and implications for surface evolution, *Science*, *284*, 1495–1503, 1999.
Strahler, A. N., Hypsometric (area-altitude) analysis of erosional topography, *Geol. Soc. Am. Bull.*, *63*, 1117–1142, 1952.
Tanaka, K. L., et al., *The Venus Geologic Mappers' Handbook*, *U.S. Geol. Surv. Open-File Rep., 94-438*, 1994.
Wise, D. U., M. P. Golombek, and G. E. McGill, Tharsis province of Mars: Geologic sequence, geometry, and a deformation mechanism, *Icarus*, *38*, 456–472, 1979.

J. Grant, Center for Earth and Planetary Studies, National Air and Space Museum, Smithsonian Institution, Washington, DC 20560, USA. (grantj@nasm.si.edu)

T. Parker, Jet Propulsion Laboratory, Mail Stop 183-501, 4800 Oak Grove Drive, Pasadena, CA 91109-8099, USA. (tparker@jpl.nasa.gov)